

Gamma echo interpreted as a phase-shift-induced transparencyGilbert R. Hoy¹ and Jos Odeurs²¹*Physics Department, Old Dominion University, Norfolk, Virginia 23529-0116*²*Katholieke Universiteit Leuven, Instituut voor Kern-en Stralingsfysica, Celestijnenlaan 200 D, B-3001 Leuven, Belgium*

(Received 16 March 2000; published 22 January 2001)

In the gamma-echo technique a radioactive source is moved, with respect to a nuclear-resonant absorber, during the lifetime of first-excited nuclear state. This introduces a phase shift between the source radiation and the radiation from the absorber. If the source is moved abruptly, introducing a pi phase shift, the time-dependent intensity shows a sharp increase in the intensity at that time, the “gamma echo.” Using the recently developed one-dimensional quantum-mechanical model, based on the technique developed by Heitler and Harris, the gamma-echo effect is seen to be a phase-shift-induced transparency. A closed-form solution for the time-dependent transmitted intensity has been obtained. The solution has the form of a sum over coherent paths that the radiation takes in going from the radioactive source through the absorber to the detector. The model shows that the sharp increase in the intensity, the “gamma echo,” at the time when the source is moved abruptly is due to constructive interference, starting at that time, between the source radiation and the radiation from the absorber. The exact form of the gamma-echo spectrum depends on the movement of the source. Shapes having multiple peaks are possible. All shapes can be found using the one-dimensional model.

DOI: 10.1103/PhysRevB.63.064301

PACS number(s): 76.80.+y, 78.90.+t, 42.25.Bs

I. INTRODUCTION

A relatively new field of research is emerging called quantum nucleonics. It deals with coherence and interference effects using resonant-gamma radiation. The plan of such research is to approach the success achieved by quantum electronics in the atomic physics field. The ultimate goal would be the development of a gamma-ray laser. In order to proceed, one needs to understand nuclear resonant gamma-ray processes as completely as possible. This paper represents a small step in that direction by addressing the gamma-echo phenomenon from a new point of view.

Mössbauer¹ discovered the recoil-free emission and absorption of gamma radiation. Subsequently, the Mössbauer effect has seen application² to many branches of physics. Very soon, after Mössbauer’s discovery, time-differential transmission experiments³ were done. Interesting experimental results^{4–7} were found using the time-differential Mössbauer spectroscopic (TDMS) method. With the advent of synchrotron radiation facilities, time-differential nuclear-resonant forward-scattering measurements⁸ have also been made using synchrotron radiation as the source.

Starting in the 1980s a number of more complicated experiments^{9–12} were performed based on modification of the TDMS technique. The “gamma-echo” effect^{11,12} was observed in the early 1990s. All of the above-mentioned experiments were analyzed using the semiclassical optical model^{3,13–16} originally due to Hamermesh. More recently a generalization of the semiclassical optical model, using space-time theory,¹⁷ has been developed to address the nuclear-resonant forward-scattering problem.

The semiclassical optical model has proven to be very useful. However, the model does not usually provide a clear physical explanation of the phenomenon being studied. This perhaps explains why Helistö and co-workers^{11,12} coined the term “gamma echo” although they were quite aware that the “gamma echo” was an interference effect. It is not at all

clear that there is an “echo” involved in these experiments. The one-dimensional quantum-mechanical model provides a clear physical explanation of the “gamma-echo” phenomenon as simply due to constructive interference between coherent amplitudes.

The outline of this paper is as follows. First we give a brief review of the TDMS experimental technique. Next the one-dimensional quantum-mechanical model solution is described. Third, the model is applied to the gamma-echo effect. Finally we provide a discussion and conclusions section.

II. REVIEW OF THE TDMS TECHNIQUE

Since the gamma-echo experiments use a modification of the TDMS experimental technique, we will discuss the TDMS technique briefly in this section. In the TDMS technique, the source emits recoil-free gamma radiation and the forward-scattered radiation is observed, in delayed coincidence with respect to the formation of the first-excited state in the source, after passing through a nuclear-resonant absorber. In such experiments a precursor event signals the formation of the first-excited nuclear level that will subsequently decay to the ground state by emission of a recoil-free gamma ray. Thus a type of lifetime curve, as used in nuclear physics, is obtained. However, in this case, the resonant source radiation will interact with the resonant nuclei in the absorber before reaching the detector. The resulting time-dependent intensity curve does not have the usual exponential decay shape characterized by the lifetime of the first-excited nuclear state.

A schematic representation of the TDMS experimental technique using ⁵⁷Co is given in Fig. 1. On the left-hand side of the figure, a sketch of the experimental configuration is shown. On the right-hand side, energy level diagrams of the source and absorber nuclear energy levels are shown for the familiar case of ⁵⁷Fe. It is the 122-keV photon from the

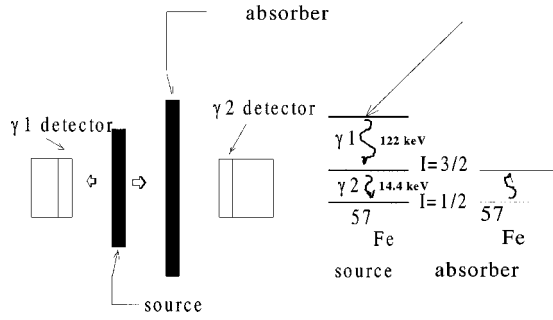


FIG. 1. A schematic summary of the TDMS technique using ^{57}Co and ^{57}Fe . On the left-hand side there is a sketch of the experimental layout. The right-hand side shows energy level diagrams for the source and absorber.

source that signals the formation of the well-known 14.4-keV Mössbauer level. The resulting 14.4-keV photon is recorded in the $\gamma 2$ detector after passing through the resonant absorber. The time-dependent intensity curve is obtained by counting the number of 14.4-keV photons recorded as a function of the time delay after the 122-keV signal photon. It is this curve that has the unusual form.

A “speed-up” effect is seen in the time-dependent intensity by observing that the initial time-dependent decay is faster than would be the case if the nuclear-resonant absorber were absent. Furthermore, at later times, for sufficiently thick absorbers, the time-dependent intensity may show local maxima, the “dynamical beat” effect. These effects are easily understood using the one-dimensional model as explained below.

III. REVIEW OF THE ONE-DIMENSIONAL QUANTUM-MECHANICAL MODEL

As noted above a one-dimensional quantum-mechanical model^{18,19} has been developed that gives a clear physical picture of nuclear-resonant forward scattering. In this section we present a brief description of the model. The model begins by using ordinary time-dependent quantum mechanics. The states of the system at time $t=0$ are taken to be the eigenstates of the Hamiltonian not including the interaction causing transitions between the nuclear levels. The general state of the system at time $t=t$ is then formed by taking a linear combination of these states with time-dependent coefficients as shown in Eq. (1). The time-dependent coefficients are due to the interaction that causes the transitions between the nuclear levels:

$$|\Psi(t)\rangle = \sum_l a_l(t) e^{-iE_l t/\hbar} |\varphi_l(0)\rangle. \quad (1)$$

Solving the Schrödinger equation leads to a set of coupled differential equations relating the expansion coefficients $a_l(t)$:

$$i\hbar \frac{da_l}{dt} = \sum_q a_q(t) e^{i(\omega_l - \omega_q)t} \langle \varphi_l(0) | V | \varphi_q(0) \rangle + i\hbar \delta_{ln} \delta(t), \quad (2)$$

where $\omega_l - \omega_q = (E_l - E_q)/\hbar$, δ_{ln} is a Kronecker delta that equals one when $l=n$ and zero otherwise, and $\delta(t)$ is a Dirac delta function. The Kronecker delta is used to satisfy the initial conditions, and the Dirac delta function is needed to take care of the discontinuity that occurs at time $t=0$ when the time axis is extended to negative values. Next the Fourier transform is introduced,

$$a_l(t) = -\frac{1}{2\pi i} \int_{-\infty}^{\infty} d\omega A_l(\omega) e^{i(\omega_l - \omega)t}. \quad (3)$$

Equation (2) can now be rewritten in the frequency domain using the technique due to Heitler,^{20,21}

$$(\omega - \omega_l + i\varepsilon) A_l(\omega) = \sum_q A_q(\omega) \frac{V_{lq}}{\hbar} + \delta_{ln}, \quad (4)$$

where V_{lq} is the matrix element inducing a transition from the q th nuclear level to the l th nuclear level state, and a pole is introduced into the lower half of the complex plane ($\varepsilon > 0$) to ensure that all amplitudes $a_l(t)$ are zero for $t < 0$.

In the model, we introduce a source nucleus and represent the absorber as a linear chain of “effective” nuclei. The reason for saying “effective” nuclei is discussed in Ref. 18 and briefly below. With these assumptions the relevant amplitudes are $A(\omega)$ the amplitude for finding the source nucleus, situated at the origin of the coordinate system, excited at time $t=0$ all absorber nuclei are in the ground state and no photons or conversion electrons present, $B_k(\omega)$ the amplitude for finding all nuclei in the ground state and only a photon of wave number k and energy $\hbar\omega_k$ present, $C_m(\omega)$ the amplitude when only the absorber nucleus located at $x=x_m$ is excited and no photons or conversion electrons present, $D_p(\omega)$ the amplitude for finding a conversion electron, of momentum p , from the source nucleus present all nuclei in their ground states and no photons are present, and $E_{mp}(\omega)$ the amplitude for finding a conversion electron, of momentum p , from the absorber nucleus located at $x=x_m$ present all nuclei in their ground states and no photons are present.

Assuming that at time $t=0$ the source nucleus is excited, and substituting these amplitudes into Eq. (5) gives the following set of coupled linear equations:

$$(\omega - \omega_0 + i\varepsilon) A(\omega) = 1 + \sum_k \frac{B_k(\omega) H_k}{\hbar} + \sum_p \frac{D_p(\omega) H_p}{\hbar}, \quad (5)$$

$$(\omega - \omega_k + i\varepsilon) B_k(\omega) = \frac{A(\omega) H_k^*}{\hbar} + \sum_m \frac{C_m(\omega) H_k^*}{\hbar} e^{-ikx_m}, \quad (6)$$

$$(\omega - \omega'_0 + i\varepsilon) C_m(\omega) = \sum_k \frac{B_k(\omega) H_k}{\hbar} e^{ikx_m} + \sum_p \frac{E_{mp}(\omega) H_p}{\hbar} e^{i(p/\hbar)x_m}, \quad (7)$$

$$(\omega - \omega_p + i\varepsilon)D_p(\omega) = \frac{A(\omega)H_p^*}{\hbar}, \quad (8)$$

$$(\omega - \omega_p + i\varepsilon)E_{mp}(\omega) = \frac{C_m(\omega)H_p^*}{\hbar} e^{i(p/\hbar)x_m}, \quad (9)$$

where H_k and H_k^* are the matrix elements corresponding to absorption and emission of a photon, respectively. Notice that, for those events that do not occur at the origin of coordinates, one must insert the appropriate phase factors. Also H_p and H_p^* are the matrix elements corresponding to absorption and emission of a conversion electron, respectively. Again, the appropriate phase factors are needed.

The meaning of these equations can be made clear by considering, for example, Eqs. (5) and (6). Equation (5) governs the amplitude for finding the source nucleus excited $A(\omega)$. Since this is the case at $t=0$, that accounts for the ‘‘1’’ on the right-hand side. The source can also get to the excited state, when in the ground state, by absorbing a photon that is present. This is the meaning of the second term on the right-hand side. Similarly, when the source nucleus is in the ground state, it can be excited by absorbing its own conversion electron. Since the source nucleus is at the origin of our coordinates, no spatial phase factors are needed. On the other hand, consider Eq. (6). This is the equation describing the situation in which all nuclei are in the ground state and there is only a photon present, $B_k(\omega)$. How can this happen? The source can emit a photon; that is the meaning of the first term on the right-hand side. Also one absorber nucleus, located at x_m , can emit a photon. Now we must put in the phase factor representing the fact that this photon appears at $x=x_m$. One must allow any other absorber nucleus to do the same thing, so the summation over all absorber nuclei is needed. The other three equations can be understood in the same way. The solution to the problem is obtained by solving this set of coupled linear equations.

First we consider a standard TDMS experiment. Assume the source and absorber nuclear transitions have a single frequency and they are in exact resonance. Then, if the scattering is forward, the time-dependent amplitude $A(t)$ for recoil-free radiation reaching the detector according to the one-dimensional model¹⁸ is

$$A_{\text{recoil-free}}(t) = \sqrt{f_s \Gamma_r / 2\hbar} e^{-(\Gamma/2\hbar)t} \times e^{-i\omega_0 t} \left[1 + \sum_{n=1}^N \binom{N}{n} \left(\frac{-f_a \Gamma_r t}{2\hbar} \right)^n \frac{1}{n!} \right]. \quad (10)$$

In Eq. (10), t is the time measured from the formation of the first-excited nuclear level in the source; f_s is the recoil-free fraction in the source; Γ_r is the radiative width of the first-excited nuclear level; Γ is the full width; ω_0 is the resonant frequency; N is the ‘‘effective’’ number of resonant nuclei in the one-dimensional chain representing the absorber; the factor just to the right of the summation sign (N over n) is a binomial coefficient; and f_a is the recoil-free fraction in the

absorber. The quantity N is the only unspecified parameter in the theory. It is related to the actual absorber thickness as described below.

The first term in Eq. (10) is due to the source of the radiation itself while the second term, involving the summation, includes the absorber. Equation (10) represents a coherent sum of amplitudes corresponding to the various ‘‘indistinguishable paths’’ the recoil-free radiation can take going to the detector. The first term represents the ‘‘path’’ corresponding to the source radiation going directly to the detector. The second term takes account of the paths that correspond to multiple scattering in the absorber. Notice the single-scattering paths ($n=1$) have a π phase shift relative to the source radiation, while the double-scattering processes ($n=2$) are back in phase with the source radiation. [This is due to the presence of the minus sign in Eq. (10).] Each multiple-scattering path has a corresponding phase shift of 0 or π . We like to say, for simplicity, that the recoil-free radiation ‘‘hops’’ on and off the effective nuclei in the absorber as the radiation makes its way to the detector.

It is this phase relationship between the various ‘‘hopping’’ paths that gives rise to the observed speed-up and dynamical beat effects. To find the intensity of the radiation reaching the detector, as a function of time after the formation of the first-excited nuclear level in the source, one needs to take the absolute value squared of the total amplitude:

$$I_{\text{recoil-free}}(t) = \frac{f_s \Gamma_r}{2\hbar} e^{-(\Gamma/h)t} \left[1 + \sum_{n=1}^N \binom{N}{n} \left(\frac{-f_a \Gamma_r t}{2\hbar} \right)^n \frac{1}{n!} \right]^2. \quad (11)$$

In order to apply this result, we will consider the familiar ⁵⁷Fe case. We will assume that the source is ‘‘thin.’’ (In general the radiation coming from the source itself may show ‘‘speed-up’’ effects i.e., line broadening. This can be easily incorporated into the model.)

In this model, the absorber is represented as a one-dimensional chain of N effective nuclei. In spite of this approximation we find that the one-dimensional model gives calculated results that are identical to those obtained using the semiclassical optical model. In the semiclassical optical model one uses the actual nuclear-resonant thickness β of the absorber. The thickness parameter β is equal to $N_0 f \sigma_0 d$, where N_0 is the number of resonant nuclei/cm³, f is the recoil-free fraction, σ_0 is the maximum cross-section evaluated on resonance, and d is the thickness of the sample.

In applying the model to experimental results, the nuclear-resonant ‘‘thickness’’ N can be considered as a parameter to be adjusted to fit the data. On the other hand, it is natural to question the relationship between N and β . It is possible to find this relationship because of the numerical agreement between the two theories. The result¹⁸ is

$$N = \frac{\beta \Gamma}{2 f \Gamma_r}. \quad (12)$$

One simply uses the integer N that is closest to the value given by the right-hand side of Eq. (12).

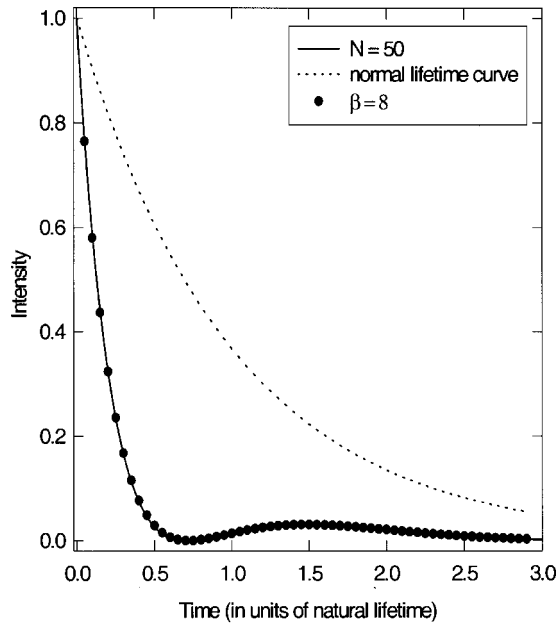


FIG. 2. The normal exponential decay of the 14.4-keV first excited state level of ^{57}Fe is shown as a dotted line. The solid curve shows the result for the time-dependent intensity of recoil-free radiation reaching the detector, after passing through a nuclear resonant absorber, according to the one-dimensional quantum mechanical model assuming $N=50$. The solid-circle curve shows the same result using the semi-classical optical model with $\beta=8$. Notice the excellent agreement using the two different theories.

A very important feature of the one-dimensional model solution is that when $n=1$, the corresponding amplitude has a minus sign. In fact it is this minus sign in the “one-hop” amplitude that is primarily responsible for the speed-up effect. The plus sign in the two-hop amplitude contributes to the dynamical beating effect.

Figure 2 shows TDMS theoretical results using the semi-classical optical model¹⁶ and the more recent one-dimensional model described here. Notice that the calculations using $N=50$ in the one-dimensional model and $\beta=8$, the actual nuclear-resonant thickness parameter, in the semi-classical optical model are in complete agreement. The normal exponential lifetime curve for the 14.4-keV level is also shown for comparison. Notice also the speed-up effect and the local maximum, at a time different from zero, which is a dynamical beat.

Figure 3 shows the first four contributing amplitudes in the one-dimensional model calculation according to Eq. (10). These four amplitudes are the “no-hop” amplitude (the solid line), the “one-hop” amplitude (the shorter dashed line), the “two-hop” amplitude (the longer dashed line), and the “three-hop” amplitude (the dash-dot line). Observe the corresponding sign for each amplitude.

IV. SOURCE MODULATION IN TDMS: THE GAMMA ECHO

As indicated above the gamma echo is produced using a TDMS technique in which the source is moved during the

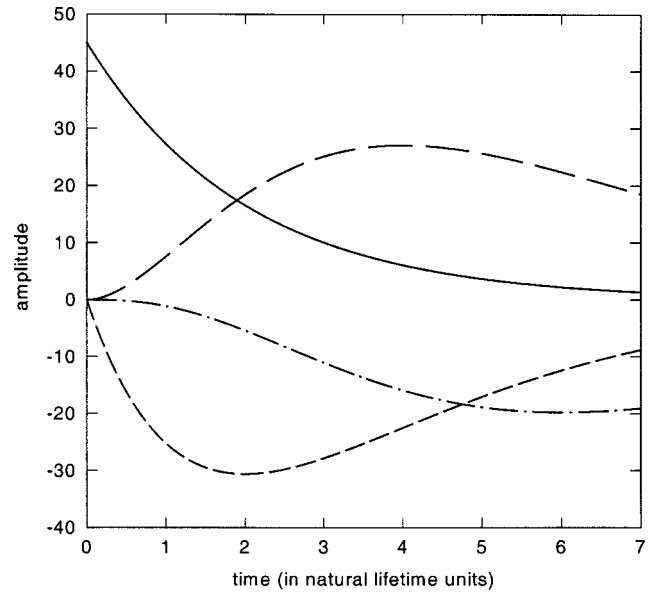


FIG. 3. The amplitudes corresponding to four of the indistinguishable paths, the source radiation takes in reaching the detector, according to Eq. (11). The solid curve shows the result for the “no-hop” case; i.e., the source radiation does not interact with the absorber. The shorter dashed curve gives the “one-hop” result where the source radiation interacts with one “effective” absorber nucleus before reaching the detector. The longer dashed curve shows the “two-hop” result, and the dashed-dot curve gives the “three-hop” result. Notice that each amplitude alternates in sign from positive to negative. This fact leads to the physical explanation of the “speed-up” and “dynamical-beat” effects.

lifetime of the first-excited nuclear state. This movement or modulation must be identical in shape and time with respect to each “signal” gamma ray, i.e., the 122-keV photon in the ^{57}Fe case. In the pioneering work of Helistö and co-workers,^{11,12} a number of different cases of source modulation were presented. Of course there are an infinite number of possibilities. We will focus on two types. First we will consider the somewhat idealized case when the source is moved instantaneously to a new position. The gamma-echo result, according to the one-dimensional theory, is very easy to predict and understand for this case. This type of source modulation, using the one-dimensional-model approach, brings out the essential features of the effect. Second, we will consider a more realistic case in which the source accelerates, rather quickly, from rest up to some velocity. The source remains moving at this velocity for some period of time and then is decelerated quickly back to rest.

A. Instantaneous source displacement

Assume that the instantaneous source displacement moves the source a distance equal to one-half of the wavelength of the source radiation. (It will be seen below that this causes the gamma echo to be a maximum. This case has been briefly treated^{22,23} recently.) The wavelength of the radiation from the 14.4-keV transition is 0.086 nm. So, now we assume that at some instant of time, after time $t=0$ during the decay of the source, the phase of the source radiation is

changed by π . This corresponds to a change in the optical-path length, from the source to the detector, by one-half the wavelength. To include this source modulation, we need to incorporate the new situation into our one-dimensional model.

The condition, that the phase of the source radiation is instantaneously changed by π at a time $t=t_{\text{switch}}$, can be treated by introducing two amplitudes. The first amplitude corresponds to the source radiating up to time t_{switch} and then changing phase. So we can write

$$A1(t) = \sqrt{f_s \Gamma_r / 2\hbar} e^{-(\Gamma/2\hbar)t} e^{-i\omega_0 t} \left[1 - \Phi(t - t_{\text{switch}}) \right] + \sum_{n=1}^N \binom{N}{n} \left(\frac{-f_a \Gamma_r t}{2\hbar} \right)^n \frac{1}{n!}. \quad (13)$$

Here $\Phi(t - t_{\text{switch}})$ is the Heaviside step function that is 0 for $t < t_{\text{switch}}$ and 1 for $t > t_{\text{switch}}$. Thus $A1(t)$ corresponds to the usual TDMS situation up to time t_{switch} when the source changes phase. The absorber continues to radiate due to its excitation by the source from time $t = 0$.

The second amplitude corresponds to the situation when the source continues radiating at time t_{switch} but now the radiation has a π -phase-shift. The second amplitude is given by

$$A2(t) = \sqrt{f_s \Gamma_r / 2\hbar} e^{-(\Gamma/2\hbar)t} e^{-i\omega_0 t} \Phi(t - t_{\text{switch}}) e^{i\pi} \times \left[1 + \sum_{n=1}^N \binom{N}{n} \left(\frac{-f_a \Gamma_r (t - t_{\text{switch}})}{2\hbar} \right)^n \frac{1}{n!} \right]. \quad (14)$$

For this second amplitude, the source has decayed to its value at time t_{switch} and continues radiating. However, the source radiation amplitude has now acquired a negative value at that time. Also the absorber continues to be excited starting from time t_{switch} . It is the interference between these two amplitudes that gives rise to the ‘‘gamma-echo’’ effect. In order to calculate the final time-dependent intensity, one adds the two amplitudes and then takes the absolute value squared,

$$I_{\pi\text{-phase-shift}}(t) = |A1(t) + A2(t)|^2. \quad (15)$$

In Fig. 4, we show the two calculated amplitudes for the ^{57}Fe case when the size of the phase shift is π . The lifetime of the nuclear first-excited state of ^{57}Fe is 141 ns. The nuclear-resonant absorber is characterized by the thickness parameter $\beta=16$ that corresponds to $N=98$ in the one-dimensional model. The time of the phase shift is fixed at 100 ns. Notice that, in Fig. 4, $A1(t)$ shows the usual initial speed-up and then at $t=t_{\text{switch}}$, the amplitude jumps to a large negative value. This is because the source amplitude is no longer canceling the amplitude of the absorber radiation. As the source continues to radiate from time t_{switch} , the amplitude has a negative value and the absorber continues to be excited. Thus $A2(t)$ has the form of a normal TDMS shape,

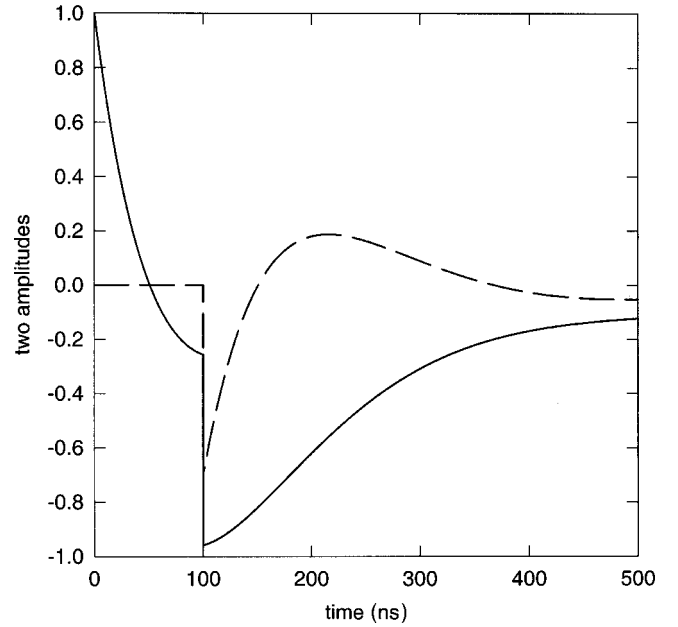


FIG. 4. The two amplitudes are shown corresponding to the case when the source is moved instantaneously a distance of one-half of the radiation wavelength. The solid curve is $A1(t)$ and the dashed curve shows $A2(t)$. Notice how the phase of $A1(t)$, just after the source is moved, is the same as that of $A2(t)$. These two amplitudes must be added to obtain the final result.

starting at time t_{switch} but now with a negative value. It is clear that, when one sums the two amplitudes and takes the absolute value squared to obtain the intensity, there is a large peak at time t_{switch} . This is shown in Fig. 5. In Fig. 5 we show the gamma-echo spectrum and the ordinary TDMS spectrum for comparison.

B. More realistic source modulation

In this section we will consider a less idealized modulation of the source. In fact, any type of source modulation can be treated using the techniques developed here. However, as outlined below, the calculation becomes cumbersome for the most general case and may tend to obscure the physics. So here we will treat the somewhat unrealistic case, where the source is at rest up to a certain time, moves at a constant velocity during some time interval, and then is again at rest.

There are several factors that need to be considered. When the source is moving at constant velocity the phase of the source radiation is changing because the optical-path length from the source to the detector is changing. Furthermore, when the source is moving at constant velocity, the source radiation is Doppler shifted in frequency relative to the resonant radiation coming from the stationary absorber. Thus we have quantum beats due to the relative phase change coming from the frequency difference between radiation coming from the moving source and the radiation coming from the stationary absorber excited by the stationary source at an earlier time.

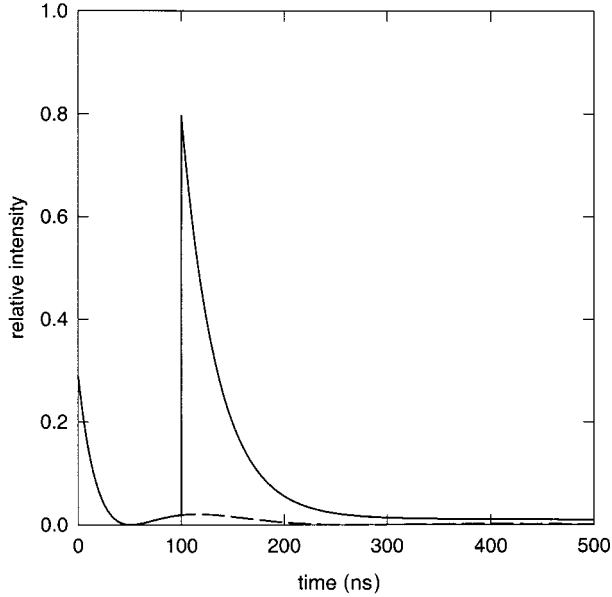


FIG. 5. The solid curve shows the “gamma-echo” spectrum. The dashed curve shows the result in the absence of the instantaneous π phase shift of the source. The two curves agree up to the time of the phase shift. Notice the increased area under the gamma-echo spectrum compared with the spectrum without the phase shift. The π phase shift causes the absorber to appear to be somewhat transparent.

Of course, when the source is moving at constant velocity, the source radiation is no longer in exact resonance with the absorber. This off-resonance effect¹⁸ has been worked out previously. However, to keep the analysis as simple as possible, we will assume that the velocity is large enough so that the source radiation is not at all in resonance with the absorber.

We assume that at some instant of time (t_{start}), after time $t=0$ during the decay of the source, the source is moved at constant velocity until a time t_{stop} when the source is brought back to rest. During this time interval, between t_{start} and t_{stop} , the source’s phase will be changing up to some maximum value depending on the source velocity and the duration of the time interval. Including this type of source modulation requires that Eq. (10) be modified. This particular source modulation can be divided into three components. For the first amplitude, the source radiates, as usual, up to time t_{start} then it starts moving. The absorber radiates due to its excitation. During the second time interval, i.e., times t_{start} to t_{stop} , the absorber continues to radiate due to its previous excitation while the source now is moving at constant velocity. The source radiation, while the source is moving, is Doppler shifted off-resonance with respect to the absorber, and radiates at the Doppler shifted frequency. During the last time interval, i.e., times greater than t_{stop} the source is at rest with a new phase determined by its final position and continues to radiate exciting the absorber again. We now have three amplitudes that contribute to the final result.

The first amplitude can be written by modifying Eq. (10) as follows:

$$A1(t) = \sqrt{f_s \Gamma_r / 2\hbar} e^{-\Gamma/2\hbar t} e^{-i\omega_0 t} \left[1 - \Phi(t - t_{\text{start}}) + \sum_{n=1}^N \binom{N}{n} \times \left(\frac{-f_a \Gamma_r t}{2\hbar} \right)^n \frac{1}{n!} \right]. \quad (16)$$

Here $\Phi(t - t_{\text{start}})$ is the Heaviside step function that is 0 for $t < t_{\text{start}}$ and 1 for $t > t_{\text{start}}$. Thus $A1(t)$ corresponds to the usual TDMS situation up to time t_{start} when the source starts moving. The absorber continues to radiate due to its excitation by the source starting at time $t=0$.

The second amplitude is given by

$$A2(t) = \sqrt{f_a \Gamma_r / 2\hbar} e^{-(\Gamma/2\hbar)t} \Phi(t - t_{\text{start}}) \times [1 - \Phi(t - t_{\text{stop}})] e^{-i\phi(t)} e^{-i\omega_0(1 + \nu/c)t}. \quad (17)$$

For this second amplitude the source radiates during the time interval between t_{start} and t_{stop} . There are now two phases that enter. We assume that the source is moved toward the absorber. There is a time-dependent phase $\phi(t)$ that is due to the shorter path length to the detector,

$$\phi(t) = \frac{2\pi}{\lambda_g} \nu(t - t_{\text{start}}), \quad (18)$$

where λ_0 is the wavelength of the resonant radiation (0.086 nm for ^{57}Fe) and ν is the source velocity. ϕ_{max} is the value when $t = t_{\text{stop}}$, see below. The second time-dependent phase arises because the moving (velocity ν) source radiation is not at the same frequency as the radiation coming from the absorber. Since we assume the source radiation is Doppler shifted off resonance, the absorber is not excited further during this period.

Finally the third amplitude is given by

$$A3(t) = \sqrt{f_s \Gamma_r / 2\hbar} e^{-(\Gamma/2\hbar)t} e^{-i\omega_0 t} \Phi(t - t_{\text{stop}}) e^{i\phi_{\text{max}}} \times \left[1 + \sum_{n=1}^N \binom{N}{n} \left(\frac{-f_a \Gamma_r (t - t_{\text{stop}})}{2\hbar} \right)^n \frac{1}{n!} \right]. \quad (19)$$

For this third amplitude, the source is again at rest radiating with its phase determined by the source’s new final position relative to the detector. The source is now able to reexcite the absorber at time t_{stop} since the source radiation is now back on resonance with respect to the absorber.

It is the interference between these three amplitudes that gives rise to the “gamma-echo” effect. In order to calculate the final time-dependent intensity, one adds the three amplitudes and then takes the absolute value squared. The explicit form of the time-dependent intensity is given in Eq. (21),

$$I_{\text{gamma echo}}(t) = |A1(t) + A2(t) + A3(t)|^2, \quad (20)$$

$$\begin{aligned}
 I_{\text{gamma echo}}(t) = & \frac{f_s \Gamma_r}{2\hbar} e^{-(\Gamma/\hbar)t} \left[\left[1 - \Phi(t - t_{\text{start}}) + \sum_{n=1}^N \binom{N}{n} \left(\frac{-f_a \Gamma_r t}{2\hbar} \right)^n \frac{1}{n!} \right] \right. \\
 & + \Phi(t - t_{\text{start}}) [1 - \Phi(t - t_{\text{stop}})] e^{-i\phi(t)} e^{-i\omega_0(v/c)t} \\
 & \left. + \Phi(t - t_{\text{stop}}) e^{i\phi_{\text{max}}} \left[1 + \sum_{n=1}^N \binom{N}{n} \left(\frac{-f_a \Gamma_r (t - t_{\text{stop}})}{2\hbar} \right)^n \frac{1}{n!} \right] \right]^2. \quad (21)
 \end{aligned}$$

In Fig. 6 we show the result for the ^{57}Fe case assuming an absorber thickness β of about 7.5 ($N=45$) and a time interval of 50 ns starting at 200 ns after the signal event. In that time interval it is assumed that the source is moving at 0.12 cm/s. The maximum phase due to position is 4.4 rad. However, notice that for $A_2(t)$ the time-dependent phase difference has two contributions, the path-length change and the quantum beat. The gamma-echo signal does not reach its maximum peak value until the phase reaches π . This makes the constructive interference, between the source radiation at that time and the absorber radiation at that time, a maximum. It is only when the source phase reaches some odd multiple of π that a maximum-sized gamma echo appears in the spectrum. In Fig. 6 the total effective phase of the source goes beyond π , but never quite reaches 3π . Thus the second ‘‘echo’’ does not attain its largest possible value. In Fig. 6 the contribution to the spectrum, from the radiation emitted from the source with recoil, is included in order to make a rough comparison with the experimental result shown in Fig. 3(c) of Ref. 11.

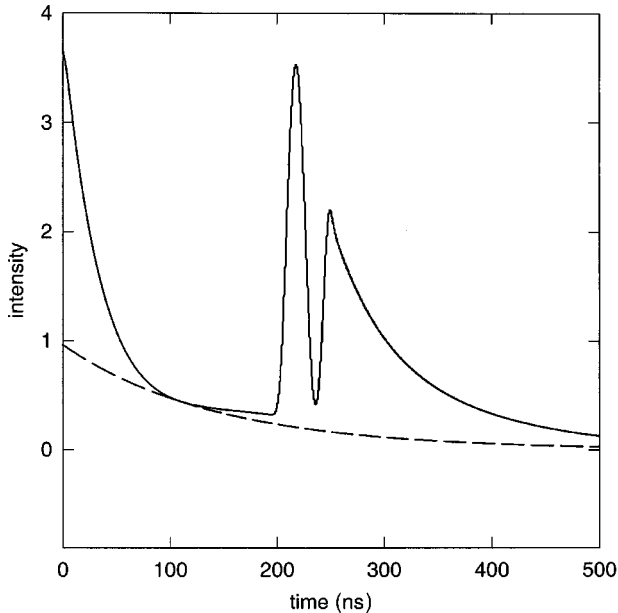


FIG. 6. The solid curve shows the result for the second type of source modulation including the background spectrum represented by the dashed curve. In this case, the phase of the source radiation has gone from zero through π up to about 2.8π . The dashed curve is the result due to the recoil radiation going through the absorber, unaffected, and reaching the detector. Compare the solid curve with an experimental result in Ref. 11.

V. DISCUSSION AND CONCLUSIONS

It is perhaps remarkable that the one-dimensional model gives results that are in such good agreement with experiment and previous theory. There are several reasons for this. In the first place, the model is not really a one-dimensional theory. One can see this in the following way. Notice that the resonant gamma radiation is treated as a plane wave, and the phase shift of the forward-scattered radiation due to a single effective nucleus is π . It is well known in x-ray diffraction²⁴ that a single resonant scattering gives a $\pi/2$ phase shift and a further $\pi/2$ phase shift arises when a summation is made over the whole plane of resonant scatterers. This result is also presented in a more appropriate context in Ref. 25. Now the model gives the π phase shift as seen by the minus sign in Eqs. (10) and (11). Thus the theory more appropriately corresponds to a nuclear-resonant sample represented by N effective parallel planes or slices.

Furthermore, it is only in the forward direction (and also in Bragg directions for single crystals) that constructive interference between the scattered waves occurs. In other directions, due to the random phases of the waves, there is destructive interference. Therefore it is only in the forward or Bragg directions that coherence needs to be considered and thus the forward-scattered radiation exhibits special features.

The one-dimensional quantum-mechanical model provides a mechanism for understanding the interaction of recoil-free gamma radiation with nuclear resonant matter. The model is physically so transparent that it is easy to understand the main features of nuclear-resonant scattering and to apply the theory to new situations, as done here for the ‘‘gamma echo.’’ It is seen that the well-known features, the ‘‘speed-up’’ and ‘‘dynamical-beat’’ effects, are due to the destructive and constructive interference between coherent amplitudes. The amplitudes that must be summed over correspond to all the indistinguishable paths the recoil-free radiation takes in going from the source through the absorber to the detector. In the theory, each path is labeled by the number of effective absorber nuclei encountered in the forward-scattering path. The number of ways each path can occur, is given by the appropriate binomial coefficient, which then weighs each path. To simplify the language, we describe the multiple recoil-free scattering processes as ‘‘hopping’’ processes. So, for example, the ‘‘no-hop’’ process corresponds to the path when the radiation goes directly from the source nucleus to the detector. For the ‘‘one-hop’’ path, the source radiation interacts with only one effective nucleus etc. The single most important result of the theory is

the fact that the odd-numbered-hop amplitudes are 180° out of phase with respect to the source radiation, while the even-numbered-hop amplitudes are in phase with the source radiation. It is interesting to note that, according to the model, it is the one-hop amplitude that is responsible for most of the absorption of radiation by an absorber.

The one-dimensional model can also explain the ‘‘gamma-echo’’ effect in terms that are physically understandable. The phenomenon is simply due to the constructive interference of coherent amplitudes. With this new interpretation, we see that there is no ‘‘echo.’’

We have considered two types of source modulation. If the source displacement is applied instantaneously, we can draw the following conclusions. The closer to $t=0$ the displacement occurs, the larger the size of the gamma-echo peak. The size of the gamma-echo peak is greatest for a source displacement that corresponds to a π phase shift in the emitted radiation. This is because the phase of the source-radiation amplitude, after the phase shift, is in phase with the amplitude of the radiation coming from the absorber that was excited previously at $t=0$.

The second type of source modulation we treat is one in which the source is initially at rest, then is moved at constant velocity and finally is brought back to rest again. In this case the source-radiation amplitude, when the source is moving, has a time-dependent phase that arises from two factors. The first factor is due to the changing path length of the source radiation to the detector. The second factor is due to the quantum beat between the radiation coming from the absorber and the Doppler-shifted radiation coming from the moving source. The resulting phase of the source-radiation amplitude, relative to the radiation from the absorber, sweeps

through a range of values. Every time the source-radiation amplitude acquires a phase that is any odd integer multiple of π , a maximum-peaked gamma echo appears in the time-dependent spectrum. In general the size, the shape, and the number of gamma-echo peaks will depend critically on the exact form of the source modulation.

A most important observation is that by applying a π phase shift to the source radiation, early in the decay of the source, one can recover a large portion of the radiation that is incident on the absorber. Thus the absorber appears to be almost transparent. So instead of speaking of a gamma echo, we prefer to say that the phenomenon is due to a π phase-shift-induced transparency. Using the new interpretation, which amounts to a sum over indistinguishable paths, it appears that certain recoil-free gamma-ray scattering paths give rise to absorption while others do not. In fact, in the usual transmission experiments, it is the ‘‘one-hop’’ paths that contribute most to absorption, while the ‘‘two-hop’’ paths do not. In the more complicated gamma-echo experiments one can say that, after the π phase shift of the source radiation, the source radiation stimulates the absorber to radiate forward. This is a type of self-stimulated emission. Without the π phase shift of the source radiation, absorption clearly takes place and the radiation reaching the detector is greatly reduced.

ACKNOWLEDGMENTS

This work was supported by the IAP-program P4-07, financed by the Belgian Federal Office for Scientific, Technical and Cultural Affairs, and by the Fonds voor Wetenschappelijk Onderzoek Vlaanderen.

-
- ¹R. L. Mössbauer, *Z. Phys.* **151**, 124 (1958).
²G. R. Hoy, *Encyclopedia of Physical Science and Technology* (Academic, New York, 1992), Vol. 10, p. 469.
³F. J. Lynch, R. E. Holland, and M. Hamermesh, *Phys. Rev.* **120**, 513 (1960).
⁴W. Neuwirth, *Z. Phys.* **197**, 473 (1966).
⁵W. Triftshäuser and P. P. Craig, *Phys. Rev.* **162**, 274 (1967).
⁶D. W. Hamill and G. R. Hoy, *Phys. Rev. Lett.* **21**, 724 (1968).
⁷G. R. Hoy and P. P. Wintersteiner, *Phys. Rev. Lett.* **28**, 877 (1972).
⁸G. V. Smirnov, *Hyperfine Interact.* **97/98**, 551 (1996).
⁹P. Hellstö, E. Ikonen, T. Katila, and K. Riski, *Phys. Rev. Lett.* **49**, 1209 (1982).
¹⁰Yu. V. Shvyd'ko, G. V. Smirnov, S. L. Popov, and T. Hertrich, *Pis'ma Zh. Eksp. Teor. Fiz.* **53**, 69 (1991) [*JETP Lett.* **53**, 69 (1991)].
¹¹P. Helistö, I. Tittonen, M. Lippmaa, and T. Katila, *Phys. Rev. Lett.* **66**, 2037 (1991).
¹²I. Tittonen, M. Lippmaa, P. Helistö, and T. Katila, *Phys. Rev. B* **47**, 7840 (1993).
¹³G. J. Perlow, *Phys. Rev. Lett.* **40**, 896 (1978).
¹⁴J. E. Monahan and G. J. Perlow, *Phys. Rev. A* **20**, 1499 (1979).
¹⁵E. Ikonen, P. Helistö, T. Katila and K. Riski, *Phys. Rev. A* **32**, 2298 (1985).
¹⁶G. R. Hoy, *Hyperfine Interact.* **107**, 381 (1997).
¹⁷Y. V. Shvyd'ko, *Phys. Rev. B* **59**, 9132 (1999).
¹⁸G. R. Hoy, *J. Phys.: Condens. Matter* **9**, 8749 (1997).
¹⁹G. R. Hoy, J. Odeurs, and R. Coussement, *Hyperfine Interact.* **120/121**, 169 (1999).
²⁰W. Heitler, *The Quantum Theory of Radiation*, 3rd ed. (Oxford University Press, Oxford, 1957), p. 164.
²¹S. M. Harris, *Phys. Rev.* **124**, 1178 (1961).
²²G. R. Hoy, J. Odeurs, and R. Coussement, *Laser Part. Beams* **18**, 1 (2000).
²³G. R. Hoy and J. Odeurs, *Proceedings of the International Conference on LASERS 99*, Quebec, Quebec, Canada, December 1999 (STS Press, McLean, VA, 2000).
²⁴R. W. James, *The Optical Principles of The Diffraction Of X-Rays* (Ox Bow, Woodbridge, CT, 1982) p. 138.
²⁵G. V. Smirnov, *Hyperfine Interact.* **123/124**, 31 (1999).